Biomechanical characterization of a desminopathy in primary human myoblasts

Navid Bonakdar [a], Justyna Luczak [a], Lena Lautscham [a], Maja Czonstke [a], Thorsten M. Koch [a], Astrid Mainka [a], Tajana Jungbauer [b], Wolfgang H. Goldmann [a,*], Rolf Schröder [b], Ben Fabry [a]

[a] Department of Physics, Friedrich-Alexander-University Erlangen-Nuremberg, Erlangen, Germany
[b] Institute of Neuropathology, University Hospital Erlangen, Erlangen, Germany

ABSTRACT

Heterozygous mutations of the human desmin gene on chromosome 2q35 cause hereditary and sporadic myopathies and cardiomyopathies. The expression of mutant desmin brings about partial disruption of the extra sarcomeric desmin cytoskeleton and abnormal protein aggregation in the sarcoplasm of striated muscle cells. The precise molecular pathways and sequential steps that lead from a desmin gene defect to progressive muscle damage are still unclear. We tested whether mutant desmin changes the biomechanical properties and the intrinsic mechanical stress response of primary cultured myoblasts derived from a patient carrying a heterozygous R350P desmin mutation. Compared to wildtype controls, undifferentiated mutant desmin myoblasts revealed increased cell death and substrate detachment in response to cyclic stretch on flexible membranes. Moreover, magnetic tweezer microrheometry of myoblasts using fibronectin-coated beads showed increased stiffness of diseased cells. Our findings provide the first evidence that altered mechanical properties may contribute to the progressive striated muscle pathology in desminopathies. We postulate that the expression of mutant desmin leads to increased mechanical stiffness, which results in excessive mechanical stress in response to strain and consecutively to increased mechanical vulnerability and damage of muscle cells.

© 2012 Elsevier Inc. All rights reserved.

1. Introduction

Mutations of the human desmin gene cause myopathies affecting skeletal and cardiac muscle. Desminopathies classically exhibit an autosomal dominant inheritance, but rare autosomal recessive cases and an increasing number of sporadic forms have been reported [1,2]. Desminopathies are usually manifest in the second to the fourth decade of life. Cardiac involvement including arrhythmias or truly dilated, hypertrophic or restrictive cardiomyopathy may precede, coincide with, or succeed skeletal muscle weakness. To date, no specific or ameliorating therapy is available [1,2]. Moreover, it is a matter of clinical debate if physical exercise has a beneficial or deteriorating effect in patients.

Desminopathies are the best-studied disease entity within the clinically and genetically heterogeneous group of myofibrillar myopathies, which are morphologically characterized by desmin-positive protein aggregates and myofibrillar changes [2]. The complex molecular pathophysiology of desminopathies seems primarily related to toxic effects of mutant desmin proteins on the formation and maintenance of the extra sarcomeric intermediate filament network. Further, mutant desmin affects essential protein–protein interactions, cell signaling cascades, mitochondrial function, and protein quality control mechanisms [3].

We previously characterized the pathological consequences of a heterozygous R350P desmin missense mutation at the clinical, myopathological, biochemical, and molecular level [4,5]. Using primary myoblasts derived from diagnostic muscle biopsies from a patient carrying a heterozygous R350P desmin mutation, we investigated to what extent the expression of mutant desmin contributes to mechanical changes and causes abnormal cellular response to mechanical perturbation. For this purpose, we adapted a biomechanical protocol that imposes cyclic mechanical strain to adherent myoblasts on flexible membranes and measured the cell viability in response to cyclic strain [6]. In addition, we performed magnetic tweezer experiments with fibronectin-coated beads to measure cell mechanical properties. Our data provide the first evidence that mutant desmin myoblasts show altered mechanical properties and higher vulnerability to mechanical stretch, which may contribute to the progressive disease process.

2. Materials and methods

2.1. Cells and cell culture

Primary human myoblasts derived from diagnostic skeletal muscle biopsies of one healthy female control and one female pa-

---

* Corresponding author. Address: Friedrich-Alexander-University of Erlangen-Nuremberg, Center for Medical Physics and Technology, Biophysics Group, Henkestrasse 91, 91052 Erlangen, Germany. Fax: +49 (0)9131 85 25601.
E-mail address: wgoldmann@biomed.uni-erlangen.de (W.H. Goldmann).

tient with a genetically proven heterozygous R350P desmin mutation were supplied from the Muscle Tissue Culture Collection (MTCC) at the Friedrich Baur Institute, Munich, Germany. Cells were cultured in skeletal muscle cell growth medium (PromoCell) supplemented with 5% PromoCell supplement Mix (PromoCell), 1.5% Glutamax (Gibco), 0.3% Gentamycin (Gibco), and 10% FCS. Immunofluorescence analysis using a monoclonal mouse antibody (Dako) directed against human desmin showed that 87% of control and 68% of mutant desmin cells stained desmin positive, thereby confirming a high number of primary myoblasts.

2.2. Cell stretcher

Stretch experiments were carried out on flexible polydimethylsiloxan (PDMS, Sylgard) substrates that were molded into the shape of a cell culture well with 2.5 cm^2 internal surface (Fig. 1A). The PDMS substrates were attached to a direct-current linear motor with an integrated gearbox (RB35, Conrad Electronic SE, Hirschau, Germany) (Fig. 1B) [7]. The substrates were then coated with 5 µg/ml fibronectin in PBS overnight at 4 °C, and 10,000 cells were seeded 24 h prior to experiments. Uniaxial, cyclic stretching was performed in the incubator under normal cell culture conditions (37 °C, 5% CO$_2$, 95% humidity) for 60 min at 30% stretch amplitude (peak-to-peak) and at a frequency of 0.25 Hz. Stretch was applied in a trapezoidal wave form at a speed of 2.5 mm/s and a resting period of 1 s between the lengthening and shortening phases.

2.3. Viability tests

To determine the number of cells before stretch, bright field and fluorescent images of Hoechst-stained cell nuclei were taken at 9 randomly chosen positions (Fig. 1C), and the (x, y) positions of the motorized microscope stage were recorded for later analysis of the same field-of-view positions. After placing the cell stretching device in the tissue culture incubator for the duration of stretch application (1 h), a live/dead staining was used to measure the cell viability. Life cells were stained with calcein-AM, and dead cells with propidium iodide as described in [6,8] (Fig. 1D). The cell stretcher was then placed back onto the microscope, the previously stored field-of-view positions were recalled, and fluorescent images were taken. The ratio of live/dead cells was analyzed using Image J software. In addition to life/dead cell counts, we also determined the number of detached cells during stretch by comparing images recorded before and after stretch. Since life/dead staining had a cytotoxic effect and led to a significantly increased cell death within 60 min (data not shown), we omitted this staining procedure prior to stretch, except in control experiments at 0% stretch condition. A minimum of 3 independent experiments were performed for each condition, with a minimum cell count of 245.

2.4. Magnetic tweezer

Magnetic tweezer microrheometry measures the cell deformation in response to magnetically generated forces. This method was used to estimate the viscoelastic cell properties both in the linear and non-linear deformation regime [9]. Super-paramagnetic 4.5 µm ⌀ epoxylated beads (Invitrogen, Karlsruhe, Germany) were coated with human fibronectin (50 µg/ml, Roche Diagnostics, Mannheim, Germany) in PBS at 4 °C for 24 h. The beads were washed in PBS and stored at 4 °C. Prior to measurements, the beads were sonicated, added to the cells (2x10^5 beads/dish), and incubated for 30 min in 5% CO$_2$ at 37 °C. A high magnetic field gradient was generated using a 2 cm long and 1 cm diameter solenoid (250 turns of a 0.4 mm diameter copper wire) with a needle-shaped high-permeability µ-metal core (HyMu80 alloy, Carpenter, Reading, PA) (Fig. 2A and B). The needle tip was placed at a distance between 20 and 30 µm from a bead bound to the cell surface (Fig. 2C) using a motorized micromanipulator (Injectman NI-2, Eppendorf, Hamburg, Germany). Bright-field images of the cell, the bead, and
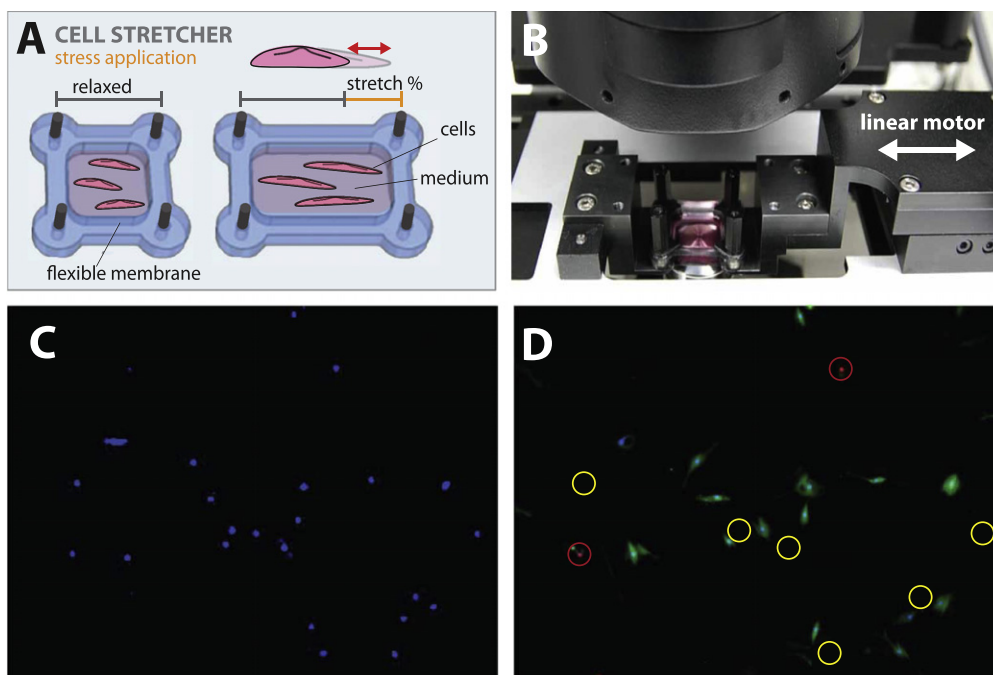

Fig. 1. Cell Stretcher. (A) Cells were plated on an elastomeric PDMS-membrane coated with the extracellular matrix-protein fibronectin. The membrane was stretched (30%) by a linear motor. (B) The stretcher was attached to an inverted microscope to observe cell behavior during stretch. The stretcher can be removed from the microscope for long-term studies in the tissue culture incubator. (C) Fluorescence image of cell nuclei stained with Hoechst taken before stretch. (D) Analysis of the identical region as in (C) after 1 h of 30% cyclic stretch. Life and dead cells are visualized with calcein-AM (green) and propidium iodide (red), respectively. Yellow circles denote the position of cells that detached during the stretch period. (For interpretation of the references to colour in this figure legend, the reader is referred to the web version of this article.)

the needle tip were taken by a charge-coupled device camera (ORCA ER, Hamamatsu, Japan) at a rate of 40 fps. The bead position was tracked using an intensity-weighted center-of-mass algorithm. A preset force was maintained by continuously updating the solenoid current or by moving the solenoid such that the needle tip-to-bead distance was kept constant (Fig. 2C). Measurements were performed at 37 °C on a heated microscope stage with an inverted microscope at 40x magnification (NA 0.6 objective) in bright-field mode. To ensure that cells had not experienced any significant forces resulting from a previous measurement, the needle was moved at least 0.5 mm between any two measurements. The total duration of measurements was limited to 30 min per dish. When a step force with an amplitude f was applied to a cell-bound bead, it moved with a displacement $d(t)$ towards the tweezer needle tip (Fig. 2D). Following [10,11], we estimated the typical strain $\gamma(t)$ as $d(t)$ divided by the bead radius r, and the typical stress σ as the applied force divided by the bead cross-sectional area, $r^2\pi$. The creep compliance $J(t)$ in units of Pa^{-1} is then given by $\gamma(t)/\sigma$ and is fit to the equation $J(t) = J_0(t/t_0)^{\beta}$ with time normalized to $t_0 = 1$ s (Fig. 2E). Because the prefactor, J_0, and the power-law exponent, β, are both force-dependent, we employed a stepwise increasing force, each force step lasting 1 s, and measured J_0 for each force level with a non-linear superposition method as described in [11]. J_0 is the creep compliance at $t_0 = 1$ s and corresponds, apart from a negligible correction factor (the Gamma function, Γ, at $1-\beta$) to the inverse magnitude of the cell's dynamic shear modulus (stiffness) evaluated at a radian frequency $\omega_0 = 1$ rad/s [12] according to $|G'(\omega_0) + iG''(\omega_0)| = 1/J_0\Gamma(1-\beta)$.

2.5. Statistical tests

Statistical significance was calculated using Student's *t*-test, assuming unequal variances. Live/death cell counts from the same day were paired. Differences between cell types or treatments were considered to be significant for $p < 0.05$.

3. Results

3.1. R350P desmin myoblasts show increased mechanical vulnerability to cyclic stretch

To investigate the response of primary human myoblasts to cyclic mechanical stretch, we cultured the cells on flexible PDMS substrates and exposed them to uniaxial cyclic stretch with a peak-to-peak amplitude of 30% at 0.25 Hz for 60 min. In time-matched control experiments (no stretch), the percentage of dead cells was around 2% in both control and diseased cells (Fig. 3A). The percentage of dead and detached cells after 1 h of cyclic 30% stretch was 10.9% in control cells and 16.6% in mutant desmin cells.

3.2. R350P desmin myoblasts show increased stiffness and baseline tension

We measured the stiffness of single myoblasts using magnetic beads that were attached to integrin cell surface receptors and laterally pulled by a magnetic tweezer device. Beads on mutant desmin cells moved significantly ($p < 0.05$) less in response to lateral force compared to control. From the bead displacements (Fig. 4A), we computed the shear modulus or stiffness of the cells. Our data show that human mutant desmin cells are approximately 2 times stiffer compared to control, regardless of the applied force magnitude (Fig. 4B). The higher stiffness indicates that mutant desmin cells have a higher baseline prestress [13,14]. This interpretation is further supported by the observation that mutant desmin cells showed a 30% increase in stiffness with increasing force, whereas controls stiffened by nearly 100%. Since the total cytoskeletal prestress is the sum of baseline prestress and externally imposed stress from the magnetically forced beads [11], cells with a higher baseline tension (desmin mutant cells) respond to increasing external forces with a smaller relative increase in stiffness (Fig. 4B).
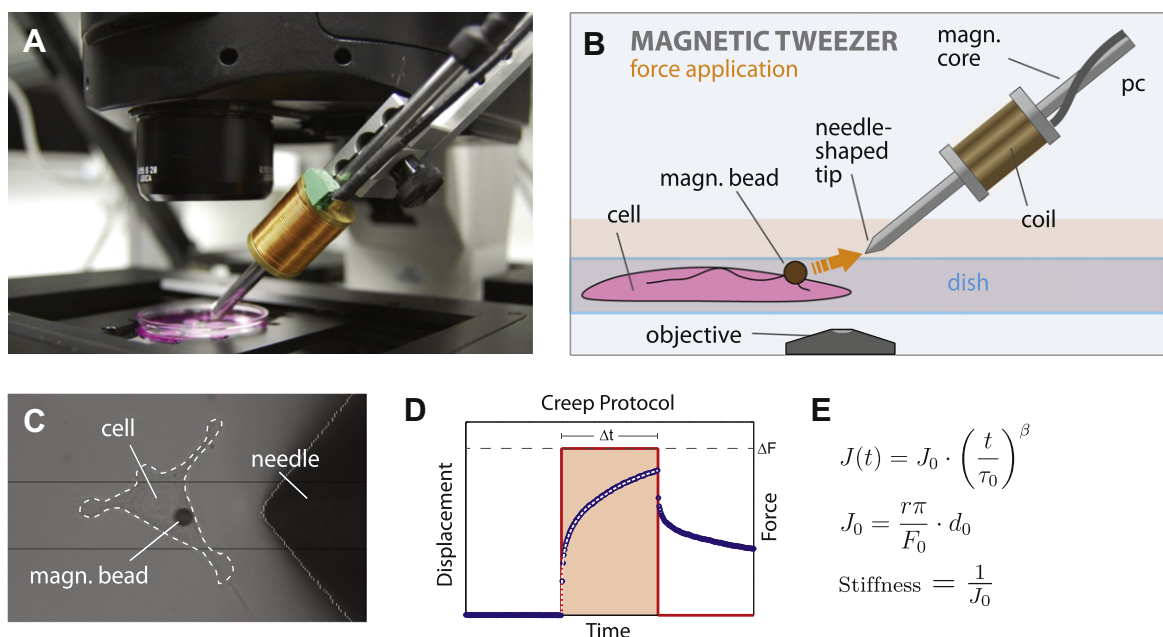

$$J(t) = J_0 \cdot \left(\frac{t}{\tau_0}\right)^{\beta}$$

$$J_0 = \frac{r\pi}{F_0} \cdot d_0$$

$$\text{Stiffness} = \frac{1}{J_0}$$

Fig. 2. Magnetic tweezer device. (A) Photographic image of the magnetic tweezer experimental setup. (B) A high magnetic field gradient is generated by a needle-shaped high-permeability core of a solenoid attached to a micromanipulator. The gradient force generated by the magnetic tweezer acts on super-paramagnetic beads coated with fibronectin. Beads are bound to the cell surface via integrin receptors which connect the extracellular space with the intracellular cytoskeleton. (C) Bright field image of the needle tip and bead attached to a cell (dashed line indicates cell contour). (D) Typical bead displacement (blue dots) in response to a single force step protocol (red line). The response was fitted by a power-law (white dashed line). (E) The power-law parameter J_0 (in units of Pa^{-1}) characterizes the elastic cell properties and corresponds to the cell's compliance (inverse of stiffness). (For interpretation of the references to colour in this figure legend, the reader is referred to the web version of this article.)
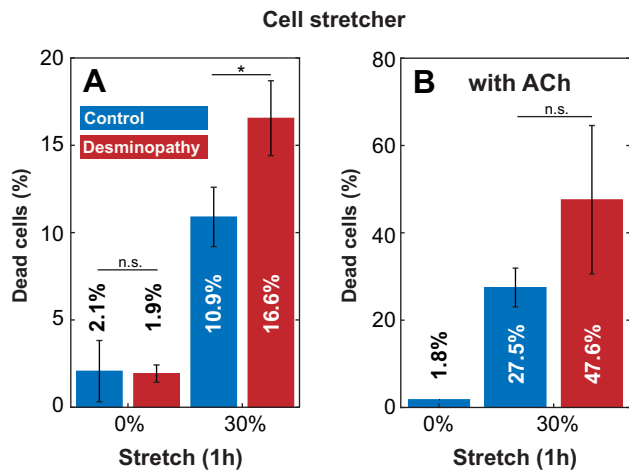
Fig. 3. Data from stretcher experiments. (A) Cyclic stretch of 30% for 1 h leads to significantly increased numbers of dead and detached cells in both control and mutant desmin cells in compared to non-stretched cells. Note, that mutant desmin cells (red, $n = 267$) are more prone to stretch-induced cell death and detachment compared to control cells (blue, $n = 406$). (B) The same experiment (after treating the cells with 0.6 mM acetylcholine (ACh)) showed higher mechanical vulnerability of both mutant desmin ($n = 245$) and control cells ($n = 284$). Unstretched but ACh-treated cells show negligible cell death. (For interpretation of the references to colour in this figure legend, the reader is referred to the web version of this article.)

3.3. Increased mechanical vulnerability to stretch is a direct consequence of increased cytoskeletal prestress and tension

According to Hooke's law, mechanical stress increases in direct proportion with stiffness and stretch amplitude. We reasoned that the higher number of detached cells and cell death after stretch in mutant desmin cells may be due to higher stretch-induced cell stress arising from higher stiffness. To test this hypothesis, we stimulated actomyosin contraction in cultured myoblasts by adding 0.6 mM acetylcholine (ACh). Since cell stiffness increases linearly with cytoskeletal prestress [14], we expected a higher fraction of dead or detached cells after ACh treatment in response to stretch. Indeed, we found in ACh-activated controls a high percentage (27.5%) of dead or detached cells after cyclic stretch, which is a 2.5-fold increase over stretched, but non-ACh-treated cells (Fig. 3A and B). In ACh-treated mutant desmin cells, the percentage of dead or detached cells after stretch increased to 47.6%, which is about a 3-fold increase over the stretched, but non-ACh-treated cells. Experiments with ACh-treated, non-stretched cells showed no significant increase in the number of dead or detached cells compared to non-stretched and non-treated controls (Fig. 3A and B).

3.4. Mutant desmin cells show high adhesiveness to the extracellular matrix

To rule out that the increased number of detached mutant desmin cells during stretch was the result of poor matrix adhesion, we applied an increasing lateral force protocol to integrin-coupled magnetic beads. This approach allowed us to record the force at
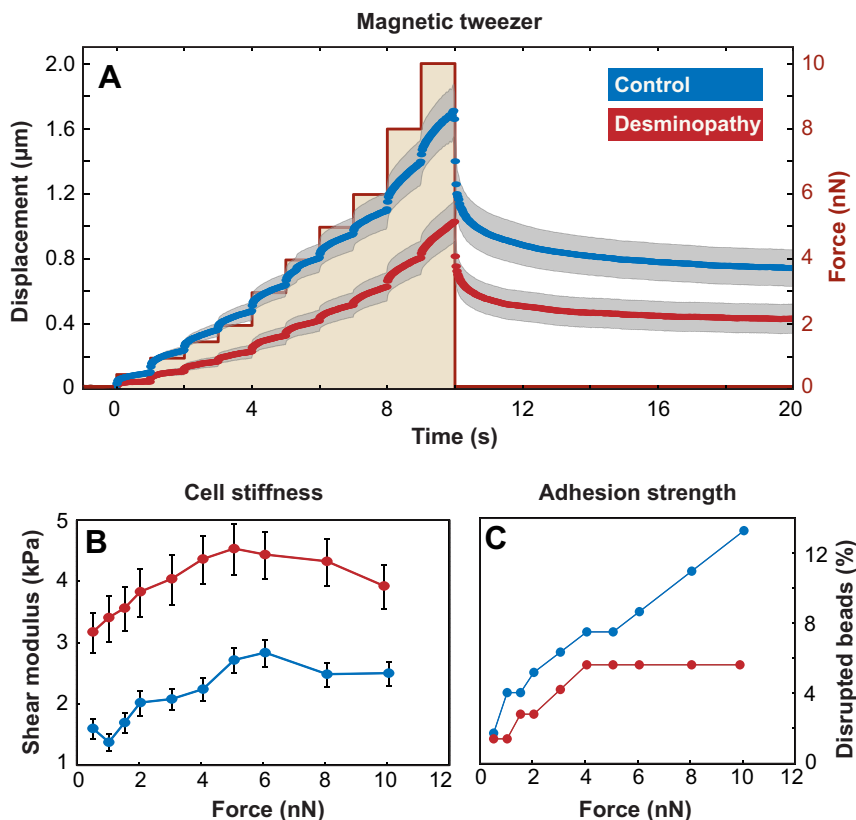

Fig. 4. Data from magnetic tweezer experiments. (A) The displacement of integrin-bound magnetic beads to stepwise increasing forces (from 0.5 to 10 nN) followed a superposition of power laws with time. Bead displacements (mean ± SE) were significantly higher in control cells (blue, $n = 150$) compared to mutant desmin cells (red, $n = 134$). (B) Shear modulus (geometric mean ± geometric SE) as a function of force showed higher stiffness of mutant desmin cells (red) compared to control cells (blue). (C) Fraction of beads that detached from the cell as a function of force. 13.3% of a total of 150 beads bound to control cells (blue) detached at a maximum force of 10 nN, while 5.6% of a total of 134 beads bound to mutant desmin cells (red) detached at a maximum force of 10 nN, indicating a higher adhesion strength in mutant desmin cells. (For interpretation of the references to colour in this figure legend, the reader is referred to the web version of this article.)

which the beads detach from the cells and to estimate the adhesion strength. The fraction of beads that detached from mutant desmin cells was lower than in control cells at all force levels (Fig. 4C), indicating that mutant desmin cells show a high adhesiveness to the extracellular matrix. We conclude that the higher number of detached mutant desmin cells was due to an increased number of cell death rather than poorer matrix adhesion properties.

4. Discussion

Higher mechanical vulnerability of skeletal muscle fibers in response to shear and pulling force during muscle contraction, especially during eccentric muscle contraction, has been previously suggested as a central mechanism for muscle fiber degeneration in a number of hereditary myopathies [15]. Since direct biomechanical assessment of human skeletal muscle fibers and tissue from diagnostic biopsies has serious technical and ethical limitations, we developed a novel approach to characterize the biomechanical properties at the level of primary human myoblasts.

Based on cell stretch and magnetic tweezer microrheology experiments, we provide evidence that pathogenic mutation-bearing myoblasts show distinct mechanical changes compared to wildtype controls. Our study focused on the pathological consequences of cells with the R350P desmin mutation that have been previously shown to exert a dominant negative effect on the ordered formation of the desmin filament system that consecutively led to abnormal protein aggregation [5].

In our experimental setting, these cells displayed higher vulnerability to mechanical stress. Compared to controls, cells expressing mutant R350P desmin were stiffer, showed increased contractile prestress, and were more susceptible to stretch-induced cell death. In keeping with Hooke's law, our data strongly indicate that the increased mechanical vulnerability of desminopathic cells is the result of higher baseline stiffness. To test the relationship between stiffness and increased cell death during stretch in more detail, we stimulated cells with ACh, which stimulates cytoskeletal actomyosin contraction and subsequently leads to increased cell stiffness [13,14]. In both, control and mutant desmin myoblasts, stretch-induced cell death and matrix detachment after ACh treatment was dramatically increased.

The idea that stiffer and more activated muscle cells are more prone to stretch-induced injury is not altogether new [16], but this has never been tested at the level of primary human myoblasts. Taken into account that desminopathies are a rare human muscle disorder, future studies on more genetically proven desminopathic cells are needed to substantiate the link between mutant desmin-induced cytoskeletal changes and altered biomechanical properties. Even from our limited data, it is tempting to speculate

that the increased biomechanical vulnerability of cells expressing mutant desmin directly contributes to the progressive muscle degeneration and weakness.

References

[1] R. Schröder, A. Vrabie, H.H. Goebel, Primary desminopathies, J. Cell Mol. Med. 11 (2007) 416–426.
[2] R. Schröder, B. Schoser, Myofibrillar myopathies: a clinical and myopathological guide, Brain Pathol. 19 (2009) 483–492.
[3] H. Bar, D. Fischer, B. Goudeau, R.A. Kley, C.S. Clemen, P. Vicart, H. Herrmann, M. Vorgerd, R. Schröder, Pathogenic effects of a novel heterozygous R350P desmin mutation on the assembly of desmin intermediate filaments in vivo and in vitro, Hum. Mol. Genet. 14 (2005) 1251–1260.
[4] I. Ferrer, M. Olive, Molecular pathology of myofibrillar myopathies, Expert Rev. Mol. Med. 10 (2008) e25.
[5] M.C. Walter, P. Reilich, A. Huebner, D. Fischer, R. Schröder, M. Vorgerd, W. Kress, C. Born, B.G. Schoser, K.H. Krause, U. Klutzny, S. Bulst, J.R. Frey, H. Lochmuller, Scapuloperoneal syndrome type Kaeser and a wide phenotypic spectrum of adult-onset dominant myopathies are associated with the desmin mutation R350P, Brain 130 (2007) 1485–1496.
[6] D.J. Tschumperlin, S.S. Margulies, Equibiaxial deformation-induced injury of alveolar epithelial cells in vitro, Am. J. Physiol. 275 (1998) L1173–1183.
[7] T. Dey, M.C. Mann, W.H. Goldmann, Comparing mechano-transduction in fibroblasts deficient of focal adhesion proteins, Biochem. Biophys. Res. Commun. 413 (2011) 541–544.
[8] V.A. Sardao, P.J. Oliveira, J. Holy, C.R. Oliveira, K.B. Wallace, Vital imaging of H9c2 myoblasts exposed to tert-butylhydroperoxide characterization of morphological features of cell death, BMC Cell Biol. 8 (2007) 11.
[9] P. Kollmannsberger, B. Fabry, High-force magnetic tweezers with force feedback for biological applications, Rev. Sci. Instrum. 78 (2007) 114301–114306.
[10] K.E. Kasza, F. Nakamura, S. Hu, P.B. Kollmannsberger, N. Bonakdar, B. Fabry, T.P. Stossel, N. Wang, D.A. Weitz, Filamin A is essential for active cell stiffening but not passive stiffening under external force, Biophys. J. 96 (2009) 4326–4335.
[11] P. Kollmannsberger, C.T. Mierke, B. Fabry, Non-linear viscoelasticity of adherent cells is controlled by cytoskeletal tension, Soft Matter 7 (2011) 3127–3132.
[12] B. Fabry, G.N. Maksym, J.P. Butler, M. Glogauer, D. Navajas, J.J. Fredberg, Scaling the microrheology of living cells, Phys. Rev. Lett. 87 (2001) 148102.
[13] A.F. Huxley, Muscle structure and theories of contraction, Prog. Biophys. Biophys. Chem. 7 (1957) 255–318.
[14] N. Wang, I.M. Tolic-Norrelykke, J. Chen, S.M. Mijailovich, J.P. Butler, J.J. Fredberg, D. Stamenovic, Cell prestress I stiffness and prestress are closely associated in adherent contractile cells, Am. J. Physiol. Cell Physiol. 282 (2002) C606–616.
[15] H. Herrmann, H. Bar, L. Kreplak, S.V. Strelkov, U. Aebi, Intermediate filaments: from cell architecture to nanomechanics, Nat. Rev. Mol. Cell Biol. 8 (2007) 562–573.
[16] R.L. Lieber, J. Friden, Muscle damage is not a function of muscle force but active muscle strain, J. Appl. Physiol. 74 (1993) 520–526.